Chinese Chemical Letters 34 (2023) 107825

Contents lists available at ScienceDirect

Chinese Chemical Letters

journal homepage: www.elsevier.com/locate/cclet

Iron-based metal–organic framework as a dual cooperative release system for enhanced vascularization and bone regeneration

Chang Xu[a], Yue Kang[b], Shiqiang Guan[a], Xufeng Dong[a,*], Daqing Jiang[b], Min Qi[a,*]

[a] School of Materials Science and Engineering, Dalian University of Technology, Dalian 116024, China
[b] Department of Breast Surgery, Cancer Hospital of China Medical University, Shenyang 110042, China

ARTICLE INFO

Article history:
Received 8 July 2022
Revised 9 September 2022
Accepted 13 September 2022
Available online 15 September 2022

Keywords:
Osteogenesis
Angiogenesis
DMOG
Metal-organic framework
Bone regeneration

ABSTRACT

Vascularization and bone regeneration are closely related in the process of bone remodeling, and designing a bioactive scaffold with pro-angiogenic and osteogenic properties may accelerate the repair of bone defects. In this work, an iron-based metal–organic framework (MIL-88) was developed as a carrier for loading a pro-angiogenic small molecular drug (dimethyloxallyl glycine, DMOG), and then embedded into the PLGA nanofibrous scaffolds to repair cranial defects in rats. Imaging and histological evaluation indicated that PLGA/MIL@D scaffold markedly enhanced vascularization and bone regeneration *in vivo*. Moreover, *in vitro* assay showed that co-delivery system significantly promoted angiogenesis by stimulating endothelial cell migration, tube formation, and enhanced osteogenesis by promoting expression of osteoblast related proteins. In addition, PLGA/MIL@D scaffold promotes angiogenesis by activating the hypoxia-inducible factor-1 (HIF-1)/vascular endothelial growth factor (VEGF) signaling pathway. Altogether, this bioactive PLGA/MIL@D scaffold can combine angiogenesis with osteogenesis, and will be a bright strategy for the repair of bone defects.

The repair and treatment of bone defects caused by trauma, infection or tumor resection remains a pressing clinical problem [1–5]. Vascularization and bone regeneration are mutually linked, and the repair and regeneration process are closely related to the formation of new blood vessels [6–10]. While common bone repair only focuses on the formation of new bone, the early vascularization is especially urgent in the process of bone formation [11,12]. The vascular network plays an integral role in maintaining the function of most tissues by providing the oxygen and nutrients needed for bone regeneration [13,14]. In contrast, the porous structure of conventional scaffolds is usually relatively simple, providing mass exchange mainly through free diffusion, making it difficult to obtain a functional vascular network [15]. Thus, a scaffold can couple of osteogenesis and angiogenesis is essential for bone tissue repair.

Dimethyloxallyl glycine (DMOG) is a cell-permeable small molecule compound that is a competitive inhibitor of prolyl hydroxylases (PHDs) [16–19]. PHDs can catalyze hydroxylation of hypoxia-inducible factor 1 (HIF-1), a key transcription factor regulating angiogenic genes, which plays a key role in angiogenesis and tissue regeneration [20,21]. Interestingly, DMOG can also promote osteogenic differentiation of bone marrow mesenchymal stem cells (BMSCs) *via* the Rho/ROCK signaling pathway [20,22]. Therefore, DMOG may serve as a promising bioactive cue for bone regeneration [23]. However, the effective loading and long-lasting release of DMOG remains a critical issue that needs to be addressed urgently.

Metal organic frameworks (MOFs) have been widely used in the medical field, and high drug loading capacity allow the carriers to synergize with drugs [24–27]. Therefore, selecting a suitable metal ion-centered MOF, which can not only serve as a drug carrier but create a favorable ionic microenvironment, may provide a promising strategy for bone regeneration [28,29]. Iron-based MOFs (*e.g.*, MIL-88) benefit from the versatility of iron ions, exhibit antibacterial, osteogenic and angiogenic effects, and occupy an important position in the field of biomaterials as well [30–32]. As a type of bioactive ion, iron is an essential component of cells with hematopoietic functions and plays a crucial role in the transport of nutrients in the blood [33,34]. On these bases, iron is often introduced into scaffolding-materials for promoting bone regeneration.

Herein, we designed a nanofibrous poly(lactic acid-*co*-glycolic acid) (PLGA) hybrid scaffold that incorporated DMOG-loaded iron-based MOFs (MIL-88) as a dual cooperative release system, which can combine the nanofibrous network mimicking the natural extracellular matrix with the drug delivery system to achieve ef-

* Corresponding authors.
E-mail addresses: dongxf@dlut.edu.cn (X. Dong), minqi@dlut.edu.cn (M. Qi).

https://doi.org/10.1016/j.cclet.2022.107825
1001-8417/

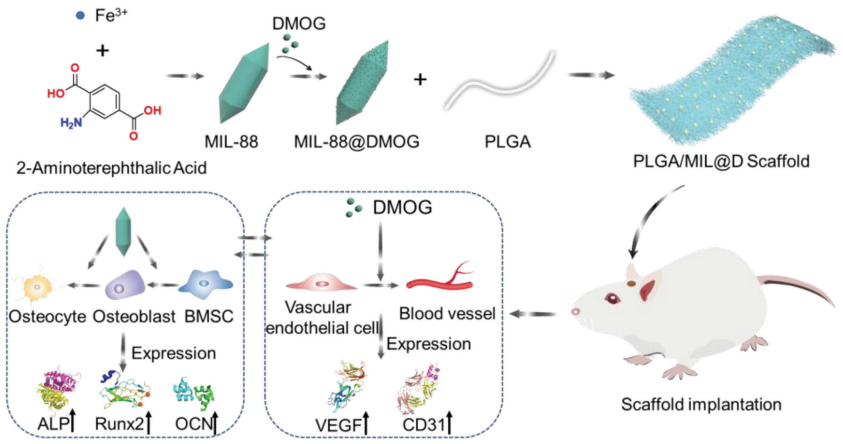

Scheme 1. Schematic illustration of the hybrid scaffold that incorporated DMOG-loaded iron-based MOFs (MIL-88) as a dual cooperative slow release system (PLGA/MIL@D) for the repair of bone defects. The well-designed scaffold was implanted into rat calvarial defect mode to evaluate the osteogenic and pro-angiogenic abilities.

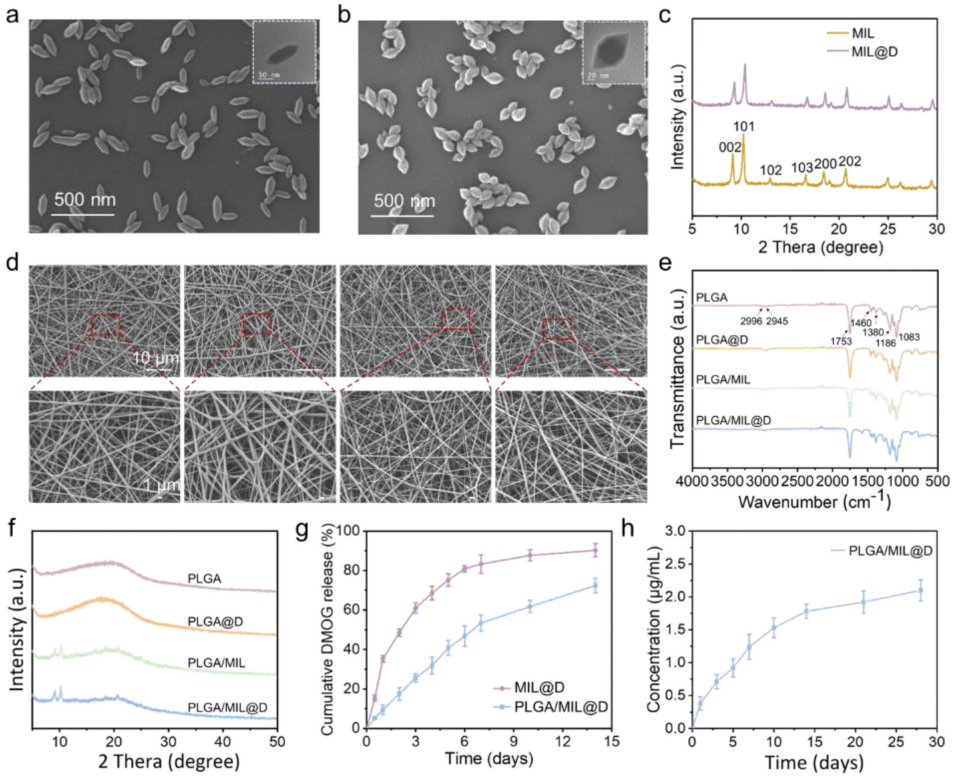

Fig. 1. Characterization of MIL, MIL@D NPs and PLGA/MIL@D scaffold. The morphologies of (a) MIL and (b) MIL@D were detected by SEM and TEM. (c) PXRD pattern of MIL and MIL@D. (d) SEM images, (e) FTIR spectra and (f) XRD curves of PLGA, PLGA@D, PLGA/MIL and PLGA/MIL@D scaffolds. (g) Cumulative release curve of DMOG in 14 days. (h) The release profiles of iron ions from PLGA/MIL@D scaffold.

fective slow release of DMOG and promote vascularization and bone regeneration (Scheme 1). The biomaterial characteristics, pro-angiogenic and osteogenic function of this composite sustained-release system were observed and evaluated in a rat cranial defect model. *In vitro* results demonstrated that PLGA/MIL@D scaffold can improve the angiogenesis and osteogenesis by activating the hypoxia-inducible factor-1 (HIF-1α)/vascular endothelial growth factor (VEGF) signaling pathway.

The introduction of MOF material enriched the drug-carrying and ion-releasing ability of the scaffold, which may be the main reason for enhancing the angiogenesis and osteoinductivity [35,36]. Scanning electron microscopy (SEM) and transmission electron microscopy (TEM) images displayed the morphology for two nanoparticles (NPs) and shown in Figs. 1a and b. The images both displayed spindle-like shape with uniform size. Notedly, the morphology after loading DMOG gradually changed from biconical rod to octahedral shape, which may be due to the introduction of DMOG more favorable to the formation of {101} facets, further accelerate the hydrolysis of iron salts and change the driving force of MIL growth [37]. And the powder X-ray diffraction (PXRD) patterns were shown in Fig. 1c, the characteristic diffraction peaks of MIL-88 appeared at about 9.2° (002), 10.3° (101), 13.1° (102), 16.7° (103), 18.5° (200) and 20.7° (202), indicating that the MIL-88 has good crystallinity. It was noteworthy that the DMOG-loaded NPs maintain an excellent crystallinity. Electrospun scaffolds are excellent candidates for tissue engineering due to their ability to mimic diversified extracellular matrix (ECM) and compositions, possessing high porosity and large surface area [38–40]. To achieve this,

DMOG, MIL-88 or MIL-88@DMOG NPs were embedded into PLGA fibrous mats by electrospinning. The morphologies of the various mats were shown in Fig. 1d. These scaffolds were randomly arranged and intertwined at the microscopic level. Besides, with the introduction of MOF, the electrospun mats gradually became much rougher compared with PLGA. The FTIR spectra were obtained to confirm the molecular structures and characteristic functional groups (Fig. 1e). The characteristic peaks of these four scaffolds resembled those of the raw PLGA, and for both PLGA/MIL and PLGA/MIL@D stents, they also had the characteristic absorption peaks of MIL-88 NPs, meaning that the chemical properties were unaffected by the electrospinning process. Moreover, the amorphous structure of PLGA was confirmed from the XRD results (Fig. 1f). Not only that, it could also be seen that MIL-88 NPs in PLGA/MIL or PLGA/MIL@D scaffolds maintain intact crystallization behavior.

Next, a polymer/drug loaded electrospun scaffold was developed to control the burst release of DMOG and iron ions in the early stage. The *in vitro* cumulative release of DMOG from MIL@D NPs and PLGA/MIL@D scaffold were shown in Fig. 1g. It could be clearly seen that the release rate of DMOG in the PLGA/MIL@D scaffold was significantly slower compared to MIL@D NPs. The effective releasing of DMOG molecules were required to cross two barriers, they should firstly release from the pores of MIL-88 NPs and subsequent diffused out from the gap of polymer fiber membrane into the medium. With the degradation of MIL-88 NPs was accelerated by the slow degradation of the polymer fiber and formed openings, so that the release rate of DMOG was also seen to be accumulated. Also, due to the slow degradation of the polymer fibers, DMOG exhibited a long-lasting slow release, which could be exceed 14 days. Further, the scaffold could provide a long-term angiogenic molecule for the bone defect. And the cumulative concentrations of the released iron ions were also determined by ICP-AES (Fig. 1h). Iron ions could be released along with the degradation of the MIL-88 NPs and PLGA fiber, reaching 1.78 μg/mL after 2 weeks. Apart from this, each group of scaffolds could be slowly degraded and absorbed after 10 weeks (Fig. S1 in Supporting informaton), which is a necessary property for tissue engineering scaffolds.

The effect of material surface microstructure and property on cell behavior was assessed by studying the adhesion and proliferation of HUVECs. The HUVECs attached to each scaffold and distributed with elongated cytoskeletons (Fig. S2 in Supporting informaton). And the shape of cell was much fuller and more regular, showing a better spreading morphology in PLGA/MIL@D group. In addition, the cell density on the surface of the scaffolds was roughly equivalent in the three groups, indicating that there was no adverse effect on cell adhesion and growth due to the addition of DMOG and MIL-88 NPs. Meanwhile, the CCK-8 assay was used to evaluate the proliferation of HUVECs on fibrous scaffolds for 7 days. According to Fig. 2a, all groups had good proliferation ability, further illustrating the excellent biocompatibility of scaffolds. Thus, the composite scaffolds were biocompatible and could serve as an adaptable attachment material for cell growth.

For bone regeneration, the early vascularization plays an important role in accelerating new bone formation [41]. To assess the ability of scaffolds to induce vascularization, a subcutaneous implantation model was performed in nude mouse for 4 weeks. And all animal studies were conducted in accordance with the Animal Care and Use Committee of China Medical University (IACUC-2,020,012). After implantation, specimens were collected that clearly reflected the formation of a vascular network around the implant (Fig. 2b), and the quantitative data was shown in Fig. S3 (Supporting information). From the digital photos, more newly formed vessels were observed within the PLGA/MIL@D stent compared to the other controls. The specific state of *in vivo* vascularization treated with this bioactive PLGA/MIL@D scaffold was further investigated by histological analysis. All results indicated that the bioactive scaffold possessed the promising vascularization and bone regeneration *in vivo*.

The ability of scaffold-mediated bone regeneration was further investigated *in vivo*. After 10-week implantation of bioactive scaffolds in the bone defects (diameter, 5 mm) of SD rats, the bone tissue corresponding to the defect areas was collected for histological and immunohistochemical examinations (Fig. 2c). As expected, more new bone formation was found in the defect area where the PLGA/MIL@D stent was implanted, and the defect area was almost covered by newly formed bone tissue. Masson staining also confirmed a higher amount of new bone tissue formation from defect edge to central area in the PLGA/MIL@D group compared with the other groups. To further explore the bone-formation and vascularization, immunohistochemical method was used to detect the expression of osteogenic (ALP, Runx2 and OCN) and angiogenic (VEGF and CD31)-related proteins in the bone implantation area and surrounding tissues (Fig. 2c). And the immunohistochemistry staining showed greater areas of ALP-, Runx2-, OCN-, VEGF- and CD31-positive cells in the PLGA/MIL@D group than in the other three groups. These results suggest that the bioactive PLGA/MIL@D scaffold enhanced the angiogenesis-osteogenesis coupling effect and further accelerated process of critical-size cranial defect repair. It indicated that DMOG is an effective stimulator for improving *in vivo* angiogenesis and that DMOG-loaded scaffolds can synergistically enhanced vascular formation.

To further determine the regulatory role of the composite scaffold, we evaluated *in vitro* human umbilical vein endothelial cells (HUVECs) migration, tube formation, and the expression of associated osteogenic proteins. The cell migration is crucial for wound healing, especially migration of HUVECs, may induce angiogenesis at the injury site and shorten the healing time. The effects of various scaffolds on HUVECs migration and tubular network formation were evaluated and the results were shown in Fig. 3a. As shown in Fig. 3a, various scaffolds demonstrated cell migration to some extent, and the migration was better in the scaffold group than in the control. In addition, the PLGA/MIL@D group had the best wound closure at 24 h, where the scratches were almost completely closed. The Transwell assay also showed the similar results, the PLGA/MIL@D group significantly promoted the migration of HUVECs, while only a limited amount of migrated HUVECs in the PLGA group. Furthermore, the tube formation assay was analyzed with the support of matrigel, capillary-like networks were formed in all groups after 24 h, and HUVECs treated by PLGA/MIL@D group formed the maximum number of branch-like structures. The semi-quantitative analyses for the wound healing, Transwell and tube formation assays were shown in Fig. S4 (Supporting information). The synergistic effect of DMOG and iron-supplying MOF could dramatically enhance *in vitro* angiogenesis of HUVECs.

To explore the effect of PLGA/MIL@D scaffold on the HIF-1α/VEGF pathway, we examined expression levels of VEGF, HIF-1α, Runx2 and OCN by using western blotting (Fig. 3b). The results suggested that DMOG-loaded scaffolds could mediate specific biological activity through upregulation of VEGF and HIF-1α protein expression. The HIF-1α pathway plays a critical role in the coupling of angiogenesis and osteogenesis. Overall, the PLGA/MIL@D scaffold could effectively release DMOG and thus exert an osteogenic function in addition to its angiogenic activity *in vitro*.

In conclusion, a novel bioactive scaffold was successfully constructed, which combine the nanofibrous network with the drug delivery system to achieve effective slow release of DMOG and bioactive ions for enhanced vascularization and bone regeneration. The PLGA/MIL@D scaffold can promote the degree of angiogenesis and mineralization at the site of bone defects in rat skull *in vivo*, which is essential for the reconstruction and regeneration of bone

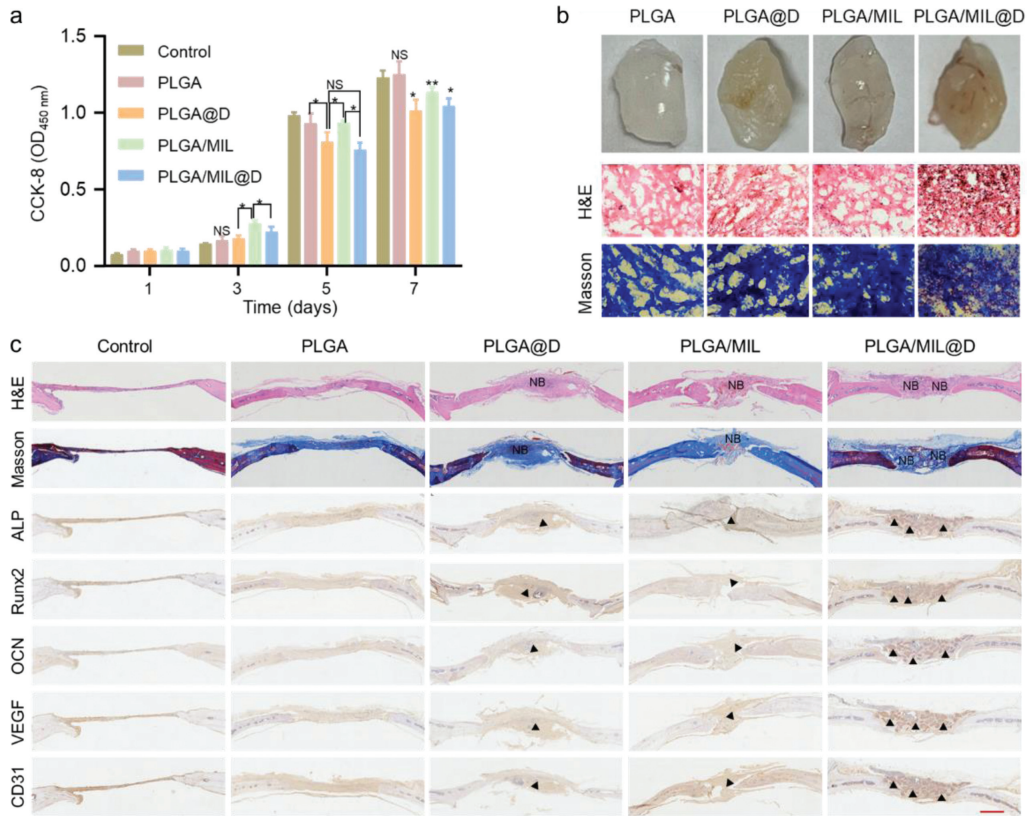

Fig. 2. The biocompatibility, osteogenic and pro-angiogenic effect of PLGA/MIL@D scaffold. (a) CCK-8 assay of HUVECs on scaffold for 1, 3, 5, 7 days ($^{*}P < 0.05$, $^{**}P < 0.01$, NS: No significance). (b) The digital photos, histological evaluation stained with H&E and Masson staining for new vessels (scale bar: 100 μm). (c) Histological evaluation stained with H&E, Masson staining and typical images of immunohistochemistry analysis of ALP, Runx2, OCN, VEGF and CD31 for new bone formation after 10 weeks. NB, new bone and triangle point to the positive staining area (scale bar: 200 μm).

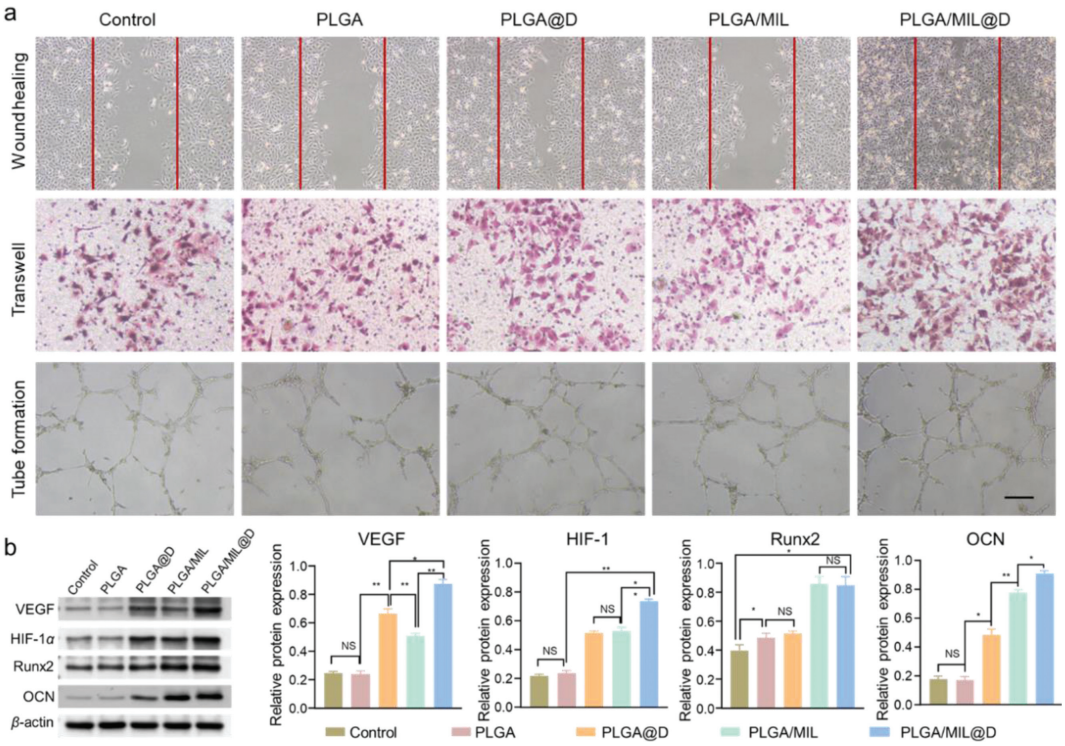

Fig. 3. (a) Representative images of wound healing assay, Transwell assay and tube formation assay for various scaffolds (scale bar: 100 μm). (b) The expression of VEGF, HIF-1α, Runx2 and OCN were examined by Western blot. NS, no significance compared to control ($n = 3$), $^{*}P < 0.05$, $^{**}P < 0.01$.

defects. *In vitro* assay showed that the composite scaffold has good biocompatibility, angiogenic and osteogenic potential. This bioactive composite scaffold can couple vascularization and osteogenesis, it would provide a new alternative for the repair of bone defects.

Declaration of competing interest

The authors declare that they have no known competing financial interests or personal relationships that could have appeared to influence the work reported in this paper.

Acknowledgment

This work was supported by the Fundamental Research Funds for the Central Universities of China (No. DUT22YG201).

Supplementary materials

Supplementary material associated with this article can be found, in the online version, at doi:10.1016/j.cclet.2022.107825.

References

[1] D. Zhao, T. Zhu, J. Li, et al., Bioact. Mater. 6 (2021) 346–360.
[2] K. Huang, G. Liu, Z. Gu, et al., Chin. Chem. Lett. 31 (2020) 3190–3194.
[3] S. Jin, X. Xia, J. Huang, et al., Acta Biomater. 127 (2021) 56–79.
[4] L. Huang, J. Zhang, X. Liu, et al., Chin. Chem. Lett. 32 (2021) 234–238.
[5] K. Huang, J. Huang, J. Zhao, et al., Chin. Chem. Lett. 33 (2022) 1941–1945.
[6] Y. Ha, X. Ma, S. Li, et al., Adv. Funct. Mater. 31 (2022) 2200011.
[7] Z. Li, S. Li, J. Yang, et al., Carbohydr. Polym. 290 (2022) 119469.
[8] T. Zhu, M. Jiang, M. Zhang, et al., Bioact. Mater. 9 (2022) 446–460.
[9] H.A. Rather, D. Jhala, R. Vasita, Mater. Sci. Eng. C 103 (2019) 109761.
[10] F. Diomede, G.D. Marconi, L. Fonticoli, et al., Int. J. Mol. Sci. 21 (2020) 3242.
[11] W. Jia, P.S. Gungor-Ozkerim, Y.S. Zhang, et al., Biomaterials 106 (2016) 58–68.
[12] X. Ye, L. Lu, M.E. Kolewe, et al., Adv. Mater. 26 (2014) 7202–7208.
[13] S. Stegen, N. van Gastel, G. Carmeliet, Bone 70 (2015) 19–27.
[14] C. Xu, Y. Chang, Y. Xu, et al., Adv. Healthc. Mater. 11 (2021) 2101911.
[15] N.A. Sears, D.R. Seshadri, P.S. Dhavalikar, et al., Tissue Eng. Part B: Rev. 22 (2016) 298–310.
[16] L. Shang, Z. Liu, B. Ma, et al., Bioact. Mater. 6 (2021) 1175–1188.
[17] S. Zippusch, K.F.W. Besecke, F. Helms, et al., Regener. Biomater. 8 (2021) 1–12.
[18] M. Zhu, S. Zhao, C. Xin, et al., Biomater. Sci. 3 (2015) 1236–1244.
[19] Q. Zhang, J.H. Oh, C.H. Park, et al., ACS Appl. Mater. Interfaces 9 (2017) 7950–7963.
[20] T. Weng, L. Zhou, L. Yi, et al., Biomed. Mater. 16 (2021) 035008.
[21] M. Shi, Y. Zhou, J. Shao, et al., Acta Biomater. 21 (2015) 178–189.
[22] H. Ding, Y.S. Gao, Y. Wang, et al., Stem Cells Dev. 23 (2014) 990–1000.
[23] H. Ding, S. Chen, W.-Q. Song, et al., Int. J. Biol. Sci. 10 (2014) 746–756.
[24] S. Zhang, X. Pei, H. Gao, et al., Chin. Chem. Lett. 31 (2020) 1060–1070.
[25] J. Liang, K. Liang, Nano Today 40 (2021) 101256.
[26] Y. Wang, J. Yan, N. Wen, et al., Biomaterials 230 (2020) 119619.
[27] J. Yang, Y.W. Yang, Small 16 (2020) 1906846.
[28] J. Li, F. Lv, J. Li, et al., Nano Res. 13 (2020) 2268–2279.
[29] M. Shyngys, J. Ren, X. Liang, et al., Front. Bioeng. Biotechnol. 9 (2021) 603608.
[30] S. Lin, X. Liu, L. Tan, et al., ACS Appl. Mater. Interfaces 9 (2017) 19248–19257.
[31] H. Shi, S. Yang, S. Zeng, et al., Appl. Mater. Today 15 (2019) 100–114.
[32] Y. Liu, T. Li, H. Ma, et al., Acta Biomater. 73 (2018) 531–546.
[33] I. Ullah, W. Zhang, L. Yang, et al., Mater. Sci. Eng. C 110 (2020) 110633.
[34] H. Shi, X. Ye, J. Zhang, et al., Bioact. Mater. 6 (2021) 1267–1282.
[35] M. Qiao, Z. Xu, X. Pei, et al., Chem. Eng. J. 434 (2022) 134583.
[36] Y. Xue, Z. Zhu, X. Zhang, et al., Adv. Healthc. Mater. 10 (2021) 2001369.
[37] B. Yang, L. Ding, H. Yao, et al., Adv. Mater. 32 (2020) 1907152.
[38] J. Ding, J. Zhang, J. Li, et al., Prog. Polym. Sci. 90 (2019) 1–34.
[39] Y. Zhang, X. Liu, L. Zeng, et al., Adv. Funct. Mater. 29 (2019) 1903279.
[40] X. Gao, S. Han, R. Zhang, et al., J. Mater. Chem. B 7 (2019) 7075–7089.
[41] J. Gu, Q. Zhang, M. Geng, et al., Bioact. Mater. 6 (2021) 3254–3268.